Size and Shape-Selective Catalysis with a Functionalized Self-Assembled Cage Host

Courtney Ngai, Bryce da Camara, Connor Z. Woods and Richard J. Hooley*

Department of Chemistry and the UC Riverside Center for Catalysis, University of California-Riverside, Riverside, CA 92521, U.S.A.

Supporting Information Placeholder

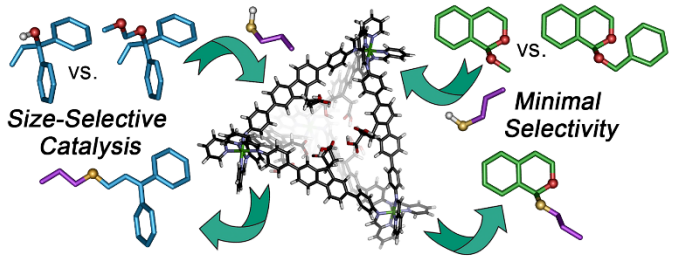

ABSTRACT: A self-assembled Fe_4L_6 cage with internally oriented carboxylic acid functions was shown to catalyze a variety of dissociative nucleophilic substitution reactions that proceed *via* oxocarbenium ion or carbocation intermediates. The catalytic behavior of the cage was compared to that of other small acid catalysts, which illustrated large differences in reactivity of the cage-catalyzed reactions, dependent on the structure of the substrate. For example, only 5% cage confers 1000-fold rate acceleration of the thioetherification of vinyldiphenylmethanol when compared to the rate with free carboxylic acid surrogates, but only a 52-fold acceleration in the formation of small thioacetals. Multiple factors control the variable reactivity in the host, including substrate inhibition, binding affinity, and accessibility of reactive groups once bound. Simple effective concentration increases or the overall charge of the cage do not explain the variations in reactivity shown by highly similar reactants in the host: small differences in structure can have large effects on reactivity. Reaction of large spherical guests is highly dependent on substitution, whereas flat guests are almost unaffected by size and shape differences. The cage is a promiscuous catalyst, but has strong selectivity for particular substrate shapes, reminiscent of enzymatic activity.

INTRODUCTION

The scope of reactivity in self-assembled synthetic hosts can be greatly expanded by introducing internally oriented functional groups to the host scaffold.[1] This concept is inspired by enzyme active sites, which show exquisite reaction control in a tight binding pocket.[2] The internal cavities in synthetic hosts cannot show the same specific size and shape matching to substrates as enzymes, so their effects on substrate reactivity are far more variable.[3] Many examples of reactivity in synthetic hosts exploit substrate recognition events that are long-lived (in molecular terms): discrete Michaelis complexes are formed that can be observed on the NMR timescale.[4] Selective coencapsulation of multiple guests confers size and shape-selectivity on the reaction,[5] and increased effective concentration can accelerate reactions.[6] When smaller unfunctionalized cages are used, the most effective reactions are often pericyclic cyclizations and rearrangements, etc.[7] The ability to coencapsulate multiple guests expands the scope of reactivity to polar, and/or organometallic processes. Catalytic cofactors such as acids,[8] bases[9] and metal complexes[10] can be coencapsulated with substrates, and accelerated reactivity, shape-selectivity and stereoselectivity can be observed.[11]

Small cavities that tightly bind guests generally show the greatest selectivity in reaction and the greatest rate accelerations.[12] However, the scope of reactivity is obviously lessened, they are more prone to substrate or product inhibition[13] and the "walls" (or "panels") of the host cannot easily be functionalized with reactive groups. Larger superstructures can be much more easily functionalized,[14] and can act as "nanophases" that contain many substrates at once.[15] Reaction scope is far wider, and the panel gaps are often larger, allowing more rapid ingress and egress from the assembly, which eases turnover. However, the internal species are not tightly bound, and the effects of large cages on substrate reactivity are less than in those that more closely mimic an "active site". The middle ground is less well-explored: medium-sized cavities that can bind multiple species, are relatively promiscuous hosts, and have reactive internal groups that are in close proximity to the bound guests.

We recently synthesized the self-assembled Fe-iminopyridine cage **1** (Figure 1),[16a] which contains carboxylic acid groups that are appended to the central fluorenyl moiety in the ligands. The cage can act as a host for neutral small molecules in organic solvents, and we have shown examples of biomimetic catalysis for polar reactions,[16] including rate accelerations,[16a,b] sequential tandem catalysis,[16a] mechanistic variations[16b] and the ability to catalyze complex, multi-step reactions.[16c] In these investigations, we found that cage **1** is quite

unusual among self-assembled host catalysts, in that it can bind multiple species on the interior, but rapid guest in/out exchange is almost always observed, which enables guest turnover and limits (in most cases) product inhibition. The guest affinities are relatively high (~10^3 – 10^5 M^{-1} in CD_3CN),[16] but the cage is a promiscuous host: virtually all substrates we have tested show some affinity for the cage (the exception being small hydrocarbons such as adamantane).[16a] The tetrahedral cage has Fe-Fe distances of 20 Å,[16a] so is not as large as some hosts,[14] but the "panel gaps" are large, and the guests are not truly encapsulated in the cavity, and most likely show significant movement when bound. As such, the activity of the host is surprising: it is far more active in acid-catalyzed processes than the free ligand analog **3**. Rate accelerations of ≥1000-fold were observed for both acetal solvolysis and alcohol thioetherifications catalyzed by **1**, when compared to the rates catalyzed by equimolar amounts of acid **3**.[16a,b]

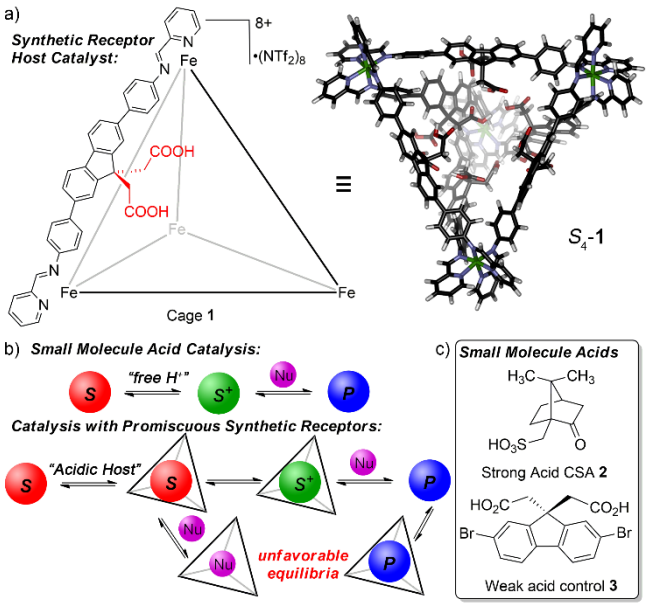

Figure 1. a) Structure of Fe_4L_6 cage **1** and a minimized structure of its S_4 isomer (SPARTAN, Hartree-Fock); b) illustration of the catalytic pathways shown by small molecule vs host acid catalysts; c) small molecule acids camphorsulfonic acid (CSA **2**) and ligand surrogate **3** controls.

While diacid **3** has the same carboxylic acid groups as the cage, the cationic nature of the assembly will obviously affect the acidity of the COOH groups in **1** somewhat. As such, we investigated other, stronger types of small molecule acids as controls as well. The anecdotal evidence suggested that the cage was about as effective a catalyst as camphorsulfonic acid **2** (CSA), which is far more acidic than the carboxylic acid groups in the cage: CSA has a pK_a of 1.2, whereas carboxylic acid **3** has a pKa ~ 3.5.[17] This observation was not consistent, however, and the scope of reaction showed by **1** was quite variable, especially upon structural changes in oxa-Pictet-Spengler reaction substrates.[16c] These differences were size- and shape-based, so could not simply be explained by the fact that the cage is cationic, so proton transfer would be more effective. There are a number of molecular recognition factors that can contribute to the differing activity of the cage to different substrates, illustrated schematically in Figure 1b. The most obvious is binding affinity, but other factors such as product and substrate inhibition must be considered, as well as the formation of unproductive ternary complexes in the host. As such, we undertook an investigation of the factors that control reactivity with cage **1**, and how reactivity varies when compared to a "comparable" acid catalyst (namely CSA **2**).

RESULTS AND DISCUSSION

The challenge when studying polar reactions with metal-ligand cage complexes is ensuring tolerance of the cage to nucleophiles, which can outcompete the reversibly coordinating ligands for the metals, disassembling the cage catalyst. As such, we focused on nucleophiles that were known to be tolerated by cage **1**, namely neutral alkanethiols and alcohols, starting with *n*-propanethiol (PrSH). The first set of electrophiles analyzed was vinyldiphenylmethanol derivatives **4a-d**, which can form multiple different substitution products and have multiple sites of reaction (especially **4c** and **4d**). The reactants were mixed in CD_3CN (15.8 mM) with 5% cage **1**, heated to 50 °C and monitored by ^1H NMR (see Supporting Information for spectra). For simplicity and to ensure accuracy, the reactions were monitored at specific times to minimize heat changes during the reaction, at 4 h and 24 h. As can be seen in Table 1, reaction of either alcohol **4a** or ether **4b** gave the conjugated, rearranged product **5** cleanly, with no addition of thiol at the quaternary center. The reaction progress was also monitored with other small molecule acids, under otherwise identical reaction conditions. CSA **2** is by far the most effective small molecule acid catalyst we tested for this process. Other small molecule acids were tested as controls, and in contrast to **1** or **2**, none are effective for the thioetherification of **4a** (see Supporting Information). Examples of other catalysts tested were 5 mol % pivalic acid, trifluoroacetic acid or tartaric acid, i.e. a simple aliphatic carboxylic acid, a strongly electron-withdrawn acid with pKa = 0.52, and a simple diacid. Using these catalysts, the observed conversions of **4a** to **5** were 1%, 6% and 2% respectively, after 4 h at 50 °C. The ligand analog **3** was even less effective, and no reaction was observed at all, even after 24 h at 80 °C. One method of mimicking the cationic nature of the cage is to combine the unfunctionalized variant of cage **1** (see Supporting Figure S-21) and ligand analog **3** using the "cofactor-mediated process" we have previously described.[16d] This is an imperfect comparison, as the host:guest possibilities are more complex, but was attempted for thoroughness. Under these conditions (see Supporting Information), only 9% conversion to **5** is seen after 24h at 50 °C: the simple presence of a cationic host does not explain the rapid reaction rate shown by cage **1** for this reaction.

Table 1. Thioetherification of Tertiary Alcohol Derivatives with Acid Catalysts

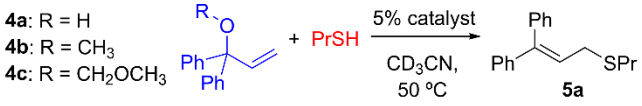

OR	% conversion, 5% cage **1**[a]		% conversion, 5% CSA **2**	
	4h	24h	4h	24 h
OH	36	88	37	82
OMe	35	75	45	>98
OMOM	19	47	64	>98

[a] [**4a-c**] = 15.8 mM, [PrSH] = 19.8 mM, [cat] = 0.8 mM, 323 K, CD_3CN.

Alcohol **4a** is an excellent example of an "optimal substrate" for cage **1**, and the thioetherification of **4a** showed essentially identical conversions with either catalyst **1** or **2**: 36% (37%) conversion was seen after 4 h, and reaction was complete after 24 h in each case; cage **1** is as active for this process as CSA. However, simply changing the leaving group from OH to OMe introduced differences between the "free" acid and the cationic host. Ethers are more basic than alcohols,[18] and **4b** reacted faster with CSA as catalyst than **4a**, with 45 % conversion after 4 h reaction time. The reactivity of **4b** in cage **1**, however, was slightly less than that of **4a** (35 % conversion after 4 h), despite the differences in "innate" reactivity. While complete conversion of **4b** was observed with CSA as catalyst after 24 h reaction time, only 75% conversion occurred with 5% cage **1**. Cage decomposition was not a factor, as the cage persisted throughout the reaction (see Figure S-18 for NMR data). To further explore the effect of changing size of electrophile on the reaction, we tested acetal derivatives of alcohol **4a**, methoxymethyl ether **4c** and tetrahydropyranyl ether **4d**. These reactants also provide an interesting window into the relative reactivity of different acid-sensitive groups in the cage. Both **4c** and **4d** have two reactive oxygen atoms that could be protonated. However, the MOM ether **4c** gave a simple reaction outcome: no evidence of oxocarbenium ion formation could be seen with either acid catalyst, and **4c** only gave product **5a**. The larger, more basic MOM group exacerbated the differences between the two catalysts, though. The reaction of **4c** catalyzed by CSA was markedly faster than that of the alcohol or ether **4a**/**4b**, with 64% conversion after 4 h at 50 °C. Reaction in cage **1** was extremely sluggish, with only 19% conversion after 4 h, and 47% conversion after 24 h. This would correspond to an initial rate difference between **4a** and **4c** of 1.9:1 in cage **1**, whereas the differences in initial rate with CSA are 0.56:1 (**4a**:**4c**).

The reactions of **4a-c** illustrate the wide range of reactivity of cage **1** between putatively "similar" substrates. At its most reactive, **1** displays the same reactivity as CSA, but simple addition of a MOM group (or a simple methyl ether) in the electrophile reduces the reactivity of the cage significantly, even taking into account increases in innate reactivity of the electrophiles.

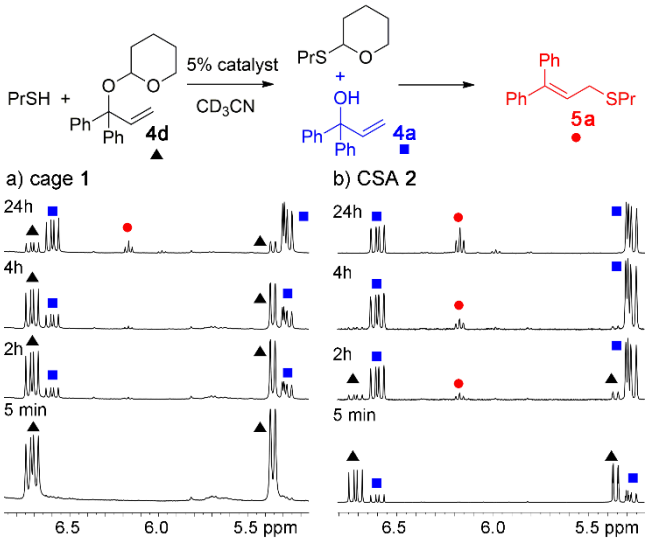

Figure 2. Expansions of the ^{1}H NMR spectra of the thioetherification of acetal **4d** over time at room temperature with a) 5% **1**; b) 5% **2** (400 MHz, 323 K, CD_3CN, [**4d**] = 15.8 mM, [PrSH] = 19.8 mM, [cat] = 0.8 mM).

While the MOM group in **4c** is not easily removed, so only one reactivity mode was observed, THP ether **4d** is far more ambiguous. The reactant displays two sites that can be protonated by acid, the THP ring O or the pendant O, and protonation at either site could lead to different bond cleavages (Table 2). Cleavage "***a***" leads to the carbocation seen in reactions of **4a-c**, whereas cleavage at the acetal center would lead to alcohol **4a** (which could then react further to form **5**) and an oxocarbenium ion intermediate. Reaction of **4d** with PrSH and either 5% **1** or **2** was performed at 23 °C to determine which reaction pathway was prevalent. Expansions of the olefinic region of the ^{1}H NMR spectra of the reactions at 23 °C are shown in Figure 2, and the differences in reactivity are immediately apparent. The THP group is lost first in both cases, forming **4a** as the initial product, but whereas CSA removes the THP very quickly (>90% at RT after 2 h), formation of the oxocarbenium ion in cage **1** is far less favorable. At 23 °C, removal of the THP group from **4d** is surprisingly slow with cage **1**: even after 24 h, complete conversion is not observed (Figure 2a). This illustrates a remarkable difference in activity between the catalysts for the initial deprotection step: whereas thioetherification of **4a** occurs at identical rates with CSA and **1**, oxocarbenium ion-based reactivity varies significantly.

To determine the effect of the THP group on the thioetherification, the reaction was monitored at higher temperatures. Table 2 shows the product distributions of reaction at 50 °C with the two different catalysts. The CSA-catalyzed reaction of **4d** with PrSH at 50 °C occurs as expected: rapid removal of the THP group (cleavage "**b**") gives alcohol **4a**, which is then converted to **5a** at essentially the same rate as described above. The THP group has minimal effect on the thioetherification reaction, as it is rapidly removed before the slow step. There is no evidence that the carbocation is formed directly from reactant **4d**. The cage-catalyzed reaction gives a much more different outcome. Despite the fact that the THP group is quite labile to acid catalysts, cage-catalyzed reaction of **4d** does not achieve complete conversion, with 5% reactant **4d** present after 21 h reaction at 50 °C. The acid-labile THP group, in essence, acts as a protecting group for the acid-catalyzed reaction. The slow reaction of THP ether **4d** concomitantly slows thioetherification of **4a**: only 66% **5a** is seen, compared with almost complete conversion of alcohol **4a** under these conditions. Interestingly, while reaction of **4d** is slower than alcohol **4a**, there appears to be no evidence for cleavage "***a***" upon treatment of **4d** with cage **1**. Alcohol **4a** is formed first, albeit slowly, and **4a** then reacts again to form **5a**.

Table 2. Oxocarbenium ion vs carbocation selectivity in thioetherification reactions of acetal **4d** at 50 °C.

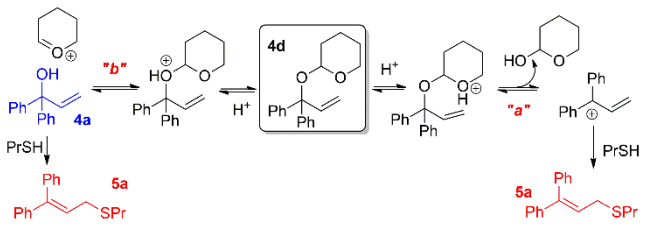

Time (h)	5% cage **1**[a]	5% CSA **2**[a]

	conv. (%)	**4a** (%)	**5** (%)	conv. (%)	**4a** (%)	**5** (%)
2	27	18	9	100	69	31
4	44	27	17	100	47	53
10	73	39	34	100	27	73
21	95	30	66	100	5	95

[a] [**4d**] = 15.8 mM, [PrSH] = 19.8 mM, [cat] = 0.8 mM, 323 K, CD_3CN.

Further analysis of the variable activation and reactivity of THP ether **4d** was performed by changing the nucleophile to water. The reactions of **4a-d** with PrSH were performed in commercial CD_3CN, with minimal precautions made to keep the reaction mixture dry, so water was present in those reactions in small amounts. However, no evidence of hydrolysis was seen in those reactions, as PrSH is a far more capable nucleophile. Electrophiles **4c** and **4d** were reacted with 6 mol.-eq. H_2O, with 5% **1** or **2** catalyst in CD_3CN as before, at either 23 °C or 50 °C, and the reactions monitored by ^1H NMR. The reactivity profile of MOM ether **4c** with water as nucleophile mirrored that with PrSH: it was quite unreactive in cage **1**, with only 19% formation of rearranged alcohol **5b** seen after 16 h at 50 °C. Further reaction was possible at 80 °C, albeit with significant cage decomposition. In contrast, with CSA, complete conversion was seen after 16 h at 50 °C, forming alcohol **5b** as major product; again, **4c** is far less reactive in cage **1** than "expected", despite **4c** being more reactive to substitution than **4a**/**4b**.

The more reactive THP ether **4d** was more informative. Reaction with 5 % cage **1** and water at 23 °C only gave deprotection of the THP group, with minimal rearrangement to form alcohol **5b** (Figure 3a). However, initial reaction with 5 % CSA was rapid, with complete deprotection of the THP group seen after ~10 mins at 23 °C. Further reaction was then observed, with two products seen: rearranged alcohol **5b**, and its THP acetal, **5c**, which is presumably formed via an acid-catalyzed reaction between cleaved THP-OH and **5b**. Interestingly, this rearranged acetal is also seen as the initial product when the reaction is performed with cage **1** (Figure 3a, labeled in purple), and even at 50 °C for 24 h, which effects complete deprotection of the THP group, minimal **5b** is formed, only **5c**. If the reaction is heated at 80 °C for 4 h, some **5b** is formed, but with significant cage decomposition.

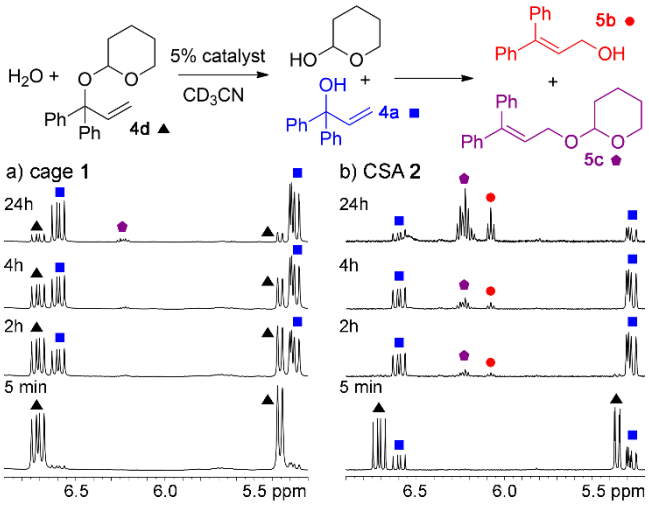

Figure 3. Expansions of the ^1H NMR spectra of the solvolysis of acetal 4d over time at room temperature with a) 5% **1**; b) 5% **2** (400 MHz, 296 K, CD_3CN, [**4d**] = 15.8 mM, [H_2O] = 95 mM, [cat] = 0.8 mM).

The outcome of these reactions is that changing the size of the electrophile changes the activity in the cage, irrespective of the "base" reactivity with a small molecule free acid. Most surprisingly, the acid-sensitive THP and MOM acetals act as a "protecting group" for acid-mediated thioetherification reactions catalyzed by cage **1**. To analyze whether the cage was simply a poor catalyst for reactions of THP ethers, we investigated the properties of a small, simple THP ether, 2-methoxytetrahydropyran **6**, in the cage. While larger guests such as **4a-d** showed size-based selectivity in reaction, with **4a** being "optimal", it was unclear how the cage would affect small electrophiles that would not properly fill the cavity. As such, we reacted **6** with 5% cage **1** or 5% CSA **2**, and four differently sized nucleophiles: *n*-propanethiol, *n*-octanethiol, *n*-dodecanethiol and water. The immediate takeaway is that the cage is a competent catalyst for reaction of THP ethers, as **6** reacts faster with 5% cage **1** and PrSH than did **4d** (after 4 h at 50 °C, 62% conversion is seen, as opposed to 27% for **4d**). Interestingly, and with both catalysts, the reactions did not go to completion, but formed an equilibrium between the two species. The equilibrium populations between methoxy acetal **6** and thioacetals **7a-7c** were essentially constant (Table 3), favoring the thioacetal in an 80:20 ratio. In contrast, hydrolysis of acetal **6** formed the lactol **7d** (with a small proportion of hydroxyaldehyde) in a 30:70 ratio, favoring starting material.

Table 3. Thioether/Ether Exchange in Small Acetal Substrates.

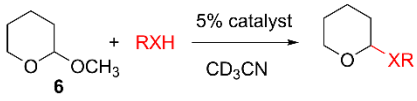

7a: XR = $S(CH_2)_2CH_3$
7b: XR = $S(CH_2)_7CH_3$
7c: XR = $S(CH_2)_{11}CH_3$
7d: XR = OH

RXH	% conversion, 4h, 5% cage **1**[a]		% conversion, 4h, 5% CSA **2**[a]	
	23°C	50°C	23°C	50°C
H_2O	28	30	28	26
PrSH	14	62	72	80
n-C_8SH	8	63	68	82
n-$C_{12}SH$	12	60	63	82

[a] [**6**] = 15.8 mM, [RSH] = 19.8 mM, [H_2O] = 95 mM, [cat] = 0.8 mM, CD_3CN.

Both cage **1** and CSA **2** catalyze the reaction and do not distort the equilibrium, as the same relative ratios of reactant:product are seen in each case. Notably, CSA **2** is a far more effective catalyst, but only for the addition of thiol nucleophiles. After 4 h at 23 °C, 72% conversion to thiol **7a** is seen, whereas with cage **1**, only 14% conversion occurs, and similar rate differences are seen with the other thiol nucleophiles. Full equilibrium can be reached after 6 h at 23 °C, or 4 h at 50 °C, whereas cage **1** requires 10 h at 50 °C. However, changing the nucleophile changes the reaction profile significantly. When water is used, equilibrium is reached after ~4 h at 23 °C with both cage **1** and CSA **2**, and no appreciable differences in reactivity are seen.

To further understand the relative reduction in activity of cage **1** with smaller electrophiles and thiol nucleophiles, a series of alkoxyisochroman derivatives **8a-e** was prepared, with varying sizes of leaving group. The reaction progress is shown in Figure 4, and the lack

of selectivity when compared to the larger guests **4a-4d** is quite remarkable. Cage **1** is capable of catalyzing the reaction, but significantly more slowly than CSA. Complete conversion is achieved after 4-6 h at 23 °C, with the secondary isoamyloxy isochroman **8d** reacting most rapidly. However, the initial rates of all 5 substrates are broadly similar, and no real size selectivity is seen. The cage-catalyzed processes are 2.7-fold slower than those with CSA, as the reaction of **8a** and PrSH catalyzed by **2** is complete after 2 h. Interestingly, the reactions of **8a-8e** show greater differences in rate with **2** (see Supporting Information for full data), as the isoamyl and benzyl reactants **8d** and **8e** were 1.5 and 2-fold more reactive than the linear alkoxy reactants **8a-8c**.

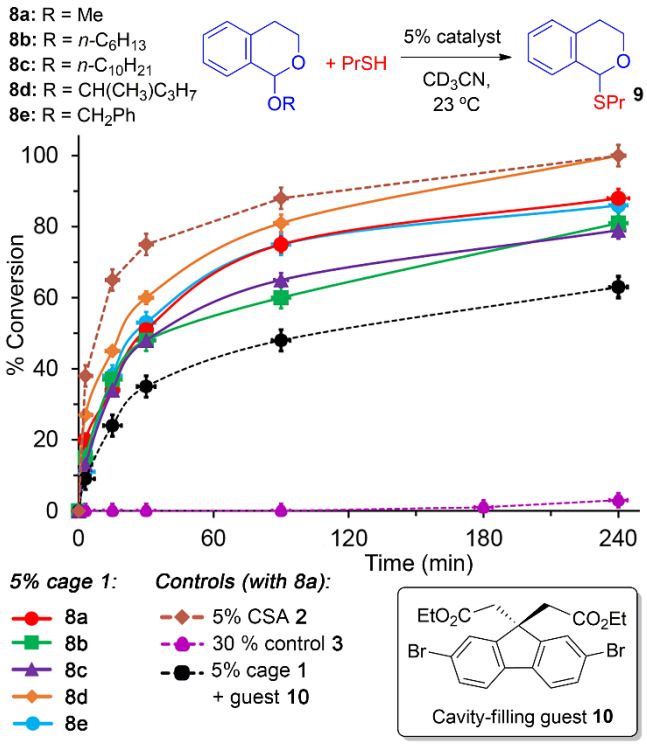

Figure 4. Reaction progress over time of the cage-catalyzed thioetherification of intermediate-sized isochromanyl ethers. [**8a-e**] = 15.8 mM, [PrSH] = 19.8 mM, [**1**,**2**] = 0.8 mM, [**3**] = 5 mM, [**10**] = 15.8 mM, 296 K, CD_3CN.

The thioetherification of **8a** was also performed with a series of control catalysts. The electrophile is sufficiently reactive to allow some conversion to occur with the ligand surrogate **3** (purple dotted line, Figure 4), although the reaction was very slow (only 3% conversion after 6 h). Still, the observable reactivity allowed a rate comparison with cage **1**, which further illustrates the relatively poor catalytic performance of cage **1** with the isochromanyl substrates. Whereas reactions of **4a** or triphenylmethanol are accelerated by >1000-fold with 5% **1** when compared to 30% **3**, only a 50-fold rate increase is observed in this case. The reaction was also performed with 5% **1** in the presence of a "blocking agent". Guest **10** binds well in the cavity, and can limit the binding and activation of reactants. As can be seen in Figure 4 (black dotted line), reaction of **8a** was significantly slowed when a competitive inhibitor was added. In the presence of 15.8 mM **10** (i.e. an amount equimolar to that of **8a**), which has an affinity $K_a = 6.9 \pm 1.2 \times 10^3\ M^{-1}$ (similar to that of **8a**), access to the cavity was limited, and the catalysis slowed. This indicates that despite the minimal size-and shape selectivity of this set of reactions, access to the active acid groups can be blocked by a competitive guest.

Overall, these results show that the relative reactivity of acid cage **1** is highly dependent on substrates. The acidity of the endohedral COOH groups is enhanced (compared to those in analog **3**, for example) by their presence in a cationic environment, but the wide variation in reactivity between ostensibly similar substrates cannot be ascribed to the overall charge of the cage. The explanation for these variations in reactivity is not immediately obvious, however. It is evident that molecular recognition effects control the reactivity, but there are multiple factors that could be involved. All of the reactions described here (and in our previous work)[16] are *catalyzed*, with only 5% cage used. The cage is a promiscuous host: all of the substrates show some affinity for the host, and they all show rapid in/out exchange. The simplest theory is that the less active reactants (i.e. **4c**, **4d**, **6**, **8a-e**) have weak affinity for the cage, so the binding affinity of the various reaction components were determined *via* UV-Vis absorption titrations. The binding constants of the guests are high enough that strong changes in absorbance of cage **1** occur at even micromolar concentrations in CH_3CN. Each guest was titrated into a 1.5 μM solution of **1** in CH_3CN, and the changes in absorbance at both 330 and 370 nm were recorded and analyzed. The binding isotherms were fit with both 1:1 and 1:2 models,[19] and the best fit for each guest determined. The results are summarized in Table 4: for the fitting curves and error analysis, see Supporting Information.

Table 4. Binding affinities (1:1 or 2:1 model) between reactants and cage **1**.[a]

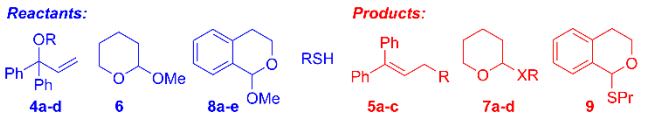

1:1 Reactant	$K_a \times 10^3\ M^{-1}$	1:1 Reactant	$K_a \times 10^3\ M^{-1}$
4a	7.4 ± 0.2	**C_8SH**	6.6 ± 0.2
4b	1.3 ± 0.06	**C_{12}SH**	7.2 ± 0.4
4c	2.9 ± 0.05	1:1 Product	$K_a \times 10^3\ M^{-1}$
4d	1.5 ± 0.09	**5a**	4.8 ± 0.4
8a	5.7 ± 0.5	**5b**	5.1 ± 0.2
8b	4.4 ± 0.3	**7a**	4.7 ± 0.06
8c	5.6 ± 0.2	**7b**	15.9 ± 0.8
8d	3.6 ± 0.1	**7c**	6.1 ± 0.08
8e	5.0 ± 0.06	**9**	2.8 ± 0.08
2:1 Guest	$K_{11} \times 10^3\ M^{-1}$	$K_{12} \times 10^3\ M^{-1}$	α ($4K_{12}/K_{11}$)
6	5.3 ± 0.07	0.009± 0.0001	0.004
7d	6.6 ± 0.3	0.77± 0.05	0.46
PrSH[16b]	114 ± 15	0.75 ± 0.008	0.026

[a] in CH_3CN, [**1**] = 3 μM, absorbance changes measured at 300 nm and 330 nm.

The binding affinities provide some explanation for the variable reactivity of electrophiles in cage **1**, but not a complete picture. While almost all the guests are small enough to allow formation of a 2:1 host:guest complex, only the smallest reactants and products show best fit to a 2:1 model. The large electrophiles and products fit

best to a 1:1 model, as expected. Amongst the electrophiles that show large variations in reactivity (i.e. **4a-4d**) the most reactive alcohol **4a** did show the greatest affinity for the cage, with K_a = 7400 M^{-1}. However, there was only a small difference in affinity between **4a** and **4b-d** (between 2.5 – 6-fold), and there was essentially no difference in affinity between **4b**, **4c** and **4d**, certainly not enough to explain the reactivity differences between **4c**/**4d** and **4a**. Electrophiles **8a-8e** all fit best to a 1:1 model, and show K_as in cage **1** between 3600 and 5700 M^{-1}. Isoamyl isochroman **8d** binds most weakly, which is consistent with its relatively sluggish reaction rate, as compared to that with CSA **2**, but the differences are modest at best. The small guests **6**, **7d** and PrSH were the only guests that favored ternary complex formation (although it is important to note that the other guests could all fit in the cavity in a 2:1 manner, but the fitting shows no preference for that mode, so the simplest assumption is that 1:1 binding if favored). Each of these guests show negative cooperativity, with α values less than 1. Notably, the electrophile guest **6** is bound far more weakly than the PrSH nucleophile.

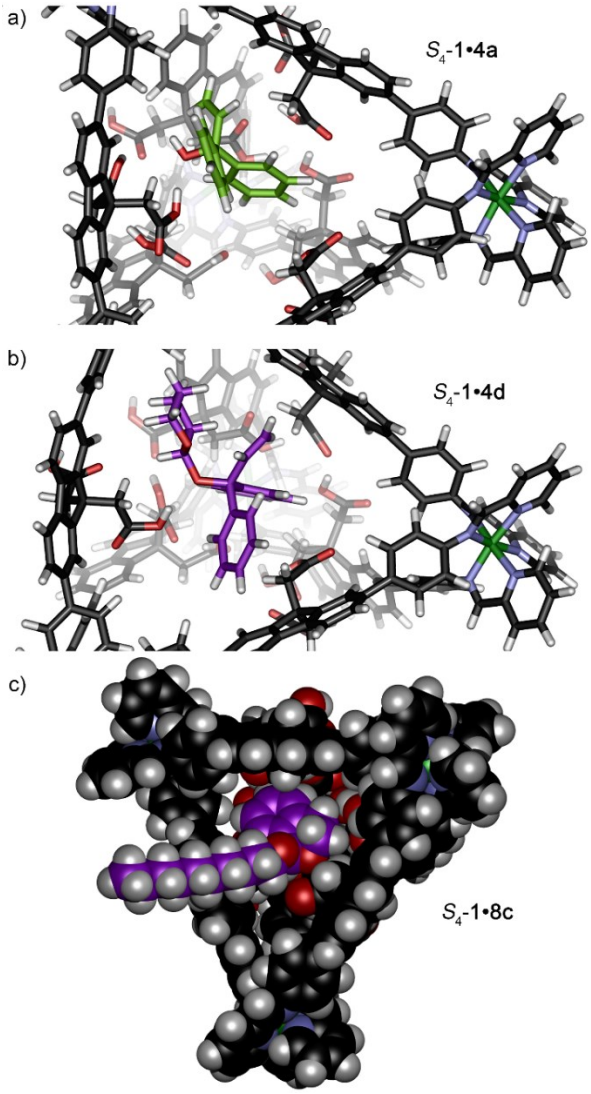

Figure 5. Expansions of the minimized structures of a) S_4-**1**•**4a**; b) S_4-**1**•**4d**. c) Minimized structure of S_4-**1**•**8c**, illustrating the protruding decyl tail (SPARTAN, Hartree-Fock).

Overall, while there are differences in affinity between the variably sized substrates and cage **1**, they are relatively small, especially considering the differences in molecular volume of the guests. The van der Waals volumes of electrophiles **4a-d** are 168, 182, 202, 235 $Å^3$ respectively, whereas **8a-c** vary from 126 to 194 to 249 $Å^3$. Doubling the overall size of the guest from **8a** to **8c** has zero effect on the affinity, within error.

Two other factors that must be considered in a catalytic process are product inhibition and substrate inhibition. The similar affinities between products and reactants illustrate why minimal product inhibition is seen: at 5% catalyst, rapid in/out exchange and ~5000 M^{-1} affinity, the product cannot prevent substrate access to the catalyst at a level sufficient to cause inhibition. Substrate inhibition is more nuanced, however. The most important observation is that the nucleophile PrSH displays a far stronger affinity for the cage than the electrophiles, and fits best to a 2:1 model. Obviously PrSH is small, and more than two molecules can easily occupy the cavity, so binding PrSH does not necessarily preclude binding electrophile as well. Substrate inhibition with PrSH appears to be a factor in the reaction of the small guest **6**. In this case, the reaction of **6** with PrSH catalyzed by cage was slowed, with respect to the reaction catalyzed by **2**, but the solvolysis reaction was not: that process occurred at broadly similar rate with 5 % **1** or **2**. The combination of forming unproductive ternary complexes with both PrSH and reactant **6** evidently slows the reaction. Substrate inhibition is only minimally disadvantageous for the other processes shown here, though, as there were few other differences in rate between thioetherification reactions and solvolyses catalyzed by **1** vs **2**. Again, the similar concentrations of nucleophile and electrophile likely minimize this inhibition pathway.

The most likely explanation for the relative lack of reactivity of **4b-4d** (compared to **4a**, which has similar reactivity as **4b** with "free" acids) is restricted *accessibility* of the -OR groups to the internal acids, once bound. Expansions of the minimized structures of S_4-**1**•**4a** and S_4-**1**•**4d** are shown in Figure 5, and illustrate the lessened "accessibility" of the basic oxygen to the internal acid groups in THP acetal **4d**, when compared to the alcohol **4a**. The cage is obviously far more bulky and hindered than a free acid, so two factors are at play when activating guests such as these. The binding event and localization of the electrophile allows rate acceleration (the reaction of **4d** in the cage is significantly faster than with free ligand **3**), but electrophiles that have more bulk around the basic oxygen (i.e. **4b-4d**) are activated less effectively than expected, even to the extent that acid-sensitive groups such as MOM and THP acts as protecting groups in acid-mediated reactions! This suggests that protonated solvent is not involved in the reaction, nor are the acids dissociated (which is plausible in CD_3CN solvent). It is likely (although not proven) that the COOH groups are the specific acid donors, and that proper orientation in the cavity is necessary for "optimal" reaction.

The cage is a promiscuous catalyst, with a "sweet spot" of reactivity. Large, spherical guests are sensitive to shape and accessibility, and show large differences in activation rate. There is some K_a dependence on reactivity, but this is not the overriding factor. In contrast, small guests that do not fill the host cavity are still activated strongly, but this activation is much less dependent on molecular recognition effects.

The lack of selectivity in the reactions of isochromans **8a-8e** is likely related to this phenomenon, as well, except in this case, the changes in size of the guest *do not* affect accessibility. As the panel gaps in the cage are large, the pendant R groups can easily protrude from the cavity once bound,[20] as shown by a minimized structure of S_4-**1**•**8c** in Figure 5c. Changes in this portion of the guest, while large in terms of overall molecular volume (**8a** = 126 Å^3, **8c** = 249 Å^3), do not have a large effect on the accessibility of the basic oxygen for the host cage. Molecular recognition effects are important, though – simply adding an equimolar amount of guest **10** to the reactions blocks the cavity and provides a 3-fold difference in rate.

Finally, these results provide an illustration of the nature of "binding" in this host. Whereas many examples of supramolecular host catalysts in the literature exploit truly encapsulated substrates, with long-lived Michaelis complexes, cage **1** behaves somewhat differently. The UV/Vis binding analysis clearly shows that the substrates have transient interactions with the cage, but the lack of an enclosed cavity suggests that there are multiple locations where these interactions can take place. The standard definition of "internal" vs. "external" binding[4b] is not really applicable when considering the accelerated reactivity of bound substrates, as the host walls do not enclose the cavity, but are oriented sideways. The intermolecular interactions that contribute to the affinity are likely a combination of van der Waals between the guests and cationic cage, with favorable H-bonding to the internal carboxylic acids also playing a role, especially for small guests such as PrSH. As can be seen by the reactions of small guests such as **6**, or flat guests such as **8a-e**, host **1** can bind and activate a wide range of species moderately effectively, but with limited selectivity. Full cavity occupancy is not necessary for reaction. The key to maximal activity is not "binding", but "productive" binding, whereby the electrophile can closely interact with the reactive groups. This is seen with guests such as triphenylmethanol or **4a**, and accelerations of ~1000-fold are seen (with respect to **3**), elevating the host's reactivity to that of a strong acid such as CSA. Those strong interactions can be easily blocked by additional substrate bulk, and the size- and shape-selectivity of the host is maximized.

CONCLUSIONS

In conclusion, we have shown that a self-assembled cage with internal functionality can catalyze a range of acid-mediated reactions, proceeding *via* multiple different cationic intermediates. The reactivity is highly variable, however, and is not solely dependent on the innate acid-sensitivity of the reactant(s). There is a delicate balance of factors that control reactivity, from the nature of the nucleophile to the size and donor accessibility of the electrophiles. The cage is a promiscuous host that can bind a wide scope of substrates with affinities on the order of 10^4 M^{-1}, and the rapid ingress and egress of guests allows turnover and effective catalysis. Neither product nor substrate inhibition are limiting factors in the reaction. The binding affinities are not the overriding factor in the catalytic selectivity, though. The cage is a promiscuous host, and observed affinities are quite similar, varying by factor of 5 at most, but large discrepancies in reactivity are observed amongst guests that bind with similar affinities. Small electrophiles react more slowly, and show minimal size-selectivity in reaction. Changing size of nucleophile or size of leaving group has a minor effect on reactivity for guests that do not fill the cavity. In contrast, optimally sized substrates show a large, up to 1000-fold rate increase (when compared to reactions catalyzed by a ligand surrogate) and at best, the cage is as active as a strong acid such as CSA. Overall, this host complex is a promiscuous acid catalyst, but has a defined set of substrate shapes that react most rapidly: it does not mimic enzyme specificity, but rather is reminiscent of non-specific fungal hydrolases, enzymes that still show strong rate acceleration, but act on a broad range of substrates.

EXPERIMENTAL

General Information. Cage **1** and weak acid control **3** were synthesized according to literature procedures.[16a] CSA **2**, 1-propanethiol, 1-octanethiol, 1-dodecanethiol, and 2-methoxytetrahydropyran **6** were purchased from Alfa Aesar or Acros Organics and used as received. Alkenes **4a**[21] and **4b**[22] as well as isochroman derivative **8a**[23] were prepared according to the known procedures. The spectral data for substrates **8e**[24] and products **5b**,[25] **7a**,[26] **7b**[27] and **7d**[28] were in agreement with literature values. ^{1}H, and ^{13}C spectra were recorded on Bruker Avance NEO 400 MHz or Bruker Avance 600 MHz NMR spectrometer. The spectrometers were automatically tuned and matched to the correct operating frequencies. Proton (^{1}H) and carbon (^{13}C) chemical shifts are reported in parts per million (δ) with respect to tetramethylsilane (TMS, δ=0), and referenced internally with respect to the protio solvent impurity for CD_3CN (^{1}H: 1.94 ppm, ^{13}C: 118.3 ppm). Deuterated NMR solvents were obtained from Cambridge Isotope Laboratories, Inc., Andover, MA, and used without further purification. Spectra were digitally processed (phase and baseline corrections, integration, peak analysis) using Bruker Topspin 1.3 and MestreNova. All other materials were obtained from Aldrich Chemical Company (St. Louis, MO), or Fisher Scientific (Fairlawn, NJ), and were used as received. Solvents were dried through a commercial solvent purification system (Pure Process Technologies, Inc.). UV/Vis spectroscopy was performed on a Cary 60 Photospectrometer using the Varian Scans program to collect data. High resolution accurate mass spectral data were obtained from the Analytical Chemistry Instrumentation Facility at the University of California, Riverside, on an Agilent 6545 QTOF LC/MS instrument.

Synthesis and Characterization of New Molecules

(1-(methoxymethyl)prop-2-ene-1,1-diyl)dibenzene (4c). Sodium hydride (60% dispersion in mineral oil, 30 mg, 1.24 mmol, 2 equiv.), was placed in a Schlenk flask with a stir bar and purged with N_2. Tetrahydrofuran (1.0 mL) was then syringed into the flask. The mixture was then stirred at room temperature for 10 minutes before 1,1-diphenylprop-2-en-1-ol (130 mg, 0.620 mmol, 1 equiv.) and bromo(methoxy)methane (85 mg, 0.682 mmol, 1.1 equiv.) was added. After 2 h, the solution was filtered to remove the NaH, the solvent was removed. The product was purified by silica column chromatography (10% EtOAc/hexane) to obtain a colorless liquid (yield: 122.9 mg, 78%). IR ($CHCl_3$): ν_{max} (cm^{-1}) 3059, 2883, 1599, 1027, 924, and 772. ^{1}H NMR (600 MHz, $CDCl_3$) δ 7.39 – 7.26 (m, 10H), 6.63 (dd, *J* = 17.2, 10.7 Hz, 1H), 5.39 (dd, *J* = 10.7, 1.2 Hz, 1H), 4.98 (dd, *J* = 17.2, 1.2 Hz, 1H), 4.76 (s, 2H), 3.42 (s, 3H); ^{13}C{^{1}H} NMR (151 MHz, $CDCl_3$) δ 143.9, 141.1, 128.0, 127.9, 127.3, 117.4, 114.9, 92.4, 55.7. HRMS (ESI-TOF) *m/z* calc[d] for $C_{17}H_{18}NaO_2$ ([M+Na]$^+$): 277.1199; found 277.1179.

2-((1,1-diphenylallyl)oxy)tetrahydro-2H-pyran (4d). p-Toluenesulfonic acid (0.53 g, 0.0031 mol, 5 mol %) was placed in a Schlenk flask with a stir bar and purged with N_2. Tetrahydrofuran (500 ml) and 1,1-diphenylprop-2-en-1-ol (13 g, 0.062 mol, 1 equiv.) was then syringed into the flask. To this solution, 4-dihydro-2H-pyran (7.8 g, 0.093 mol, 1.5 equiv.) was added, and the mixture was stirred at room temperature. After 16 h, the solution was diluted with EtOAc and washed with sat. $NaHCO_3$ and brine. The organic phase was then dried with $MgSO_4$ and concentrated in vacuo. The product was purified by silica column

chromatography (10% EtOAc/hexane) to obtain a colorless liquid (yield: 15.5 g, 85%). IR ($CHCl_3$): ν_{max} (cm^{-1}) 3025, 2942, 1608, 1075, 988, 772. ^1H NMR (600 MHz, $CDCl_3$) δ 7.43 (dd, *J* = 8.3, 1.3 Hz, 2H), 7.39 – 7.20 (m, 8H), 6.72 (dd, *J* = 17.3, 10.7 Hz, 1H), 5.37 (dd, *J* = 10.7, 1.4 Hz, 1H), 4.85 (d, *J* = 1.4 Hz, 1H), 4.83 – 4.75 (m, 1H), 4.00 (ddd, *J* = 11.5, 6.9, 4.9 Hz, 1H), 3.57 – 3.22 (m, 1H), 2.00 (ddt, *J* = 11.8, 8.8, 5.0 Hz, 1H), 1.91 – 1.60 (m, 2H), 1.73 – 1.37 (m, 3H). $^{13}C\{^1H\}$ NMR (151 MHz, $CDCl_3$) δ 144.5, 144.1, 141.7, 128.1, 127.9, 127.4, 117.5, 85.3, 62.4, 31.7, 25.5, 19.8. HRMS (ESI-TOF) *m/z* calc[d] for $C_{20}H_{22}O_2Na$ ($[M+Na]^+$): 317.1512; found 317.1501.

General procedure for isolation of products 5a, 7c, and 9: Substrate (**4a, 6, or 8a**) and CSA (43.2 mg, 186 mmol, 30 mol %), were placed in a Schlenk flask with a stir bar and purged with N_2. The substrate was then dissolved in dry CH_3CN (1.0 mL). Propanethiol (1.0 mL) was added to the flask, and the reaction was stirred at room temperature in a sand bath for 16 h. The solvent was removed and the product dried *in vacuo*. The products were purified by silica gel chromatography eluting with 0-30% EtOAc/hexane.

(3,3-diphenylallyl)(propyl)sulfane (5a). The reaction with substrate **4a** (130 mg, 0.620 mmol, 1 equiv.) afforded a colorless liquid (yield: 148.1 mg, 89%): IR (CH_3CN): ν_{max} (cm^{-1}) 3005, 2943 1631, 1375, 1038, 918, 748. ^1H NMR 400 MHz, (CD_3CN) δ 7.48 – 7.37 (m, 3H), 7.36 – 7.28 (m, 3H), 7.27 – 7.19 (m, 4H), 6.17 (t, *J* = 7.9 Hz, 1H), 3.22 (d, *J* = 7.9 Hz, 2H), 2.47 – 2.42 (m, 2H), 1.42 (dt, *J* = 14.6, 7.3 Hz, 2H), 0.90 (t, *J* = 7.3 Hz, 3H). $^{13}C\{^1H\}$ NMR (151 MHz, CD_3CN) δ 129.8, 128.3, 128.2, 127.2, 125.7, 117.0, 32.7, 30.0, 22.7, 12.6. HRMS (ESI-TOF) *m/z* calc[d] for $C_{18}H_{19}S$ ($[M-H]^-$): 267.1213; found 267.1212.

2-(dodecylthio)tetrahydro-2H-pyran (7c). The reaction with substrate **6** (102 mg, 0.620 mmol, 1 equiv.) afforded a colorless liquid (yield: 154.5 mg, 87%): IR (CH_3CN): ν_{max} (cm^{-1}) 2998, 2943, 1443, 1375, 1038, 918, 832, 751, 655. ^1H NMR (400 MHz, CD_3CN) δ 4.87 (dd, *J* = 6.3, 3.8 Hz, 1H), 4.01 (dt, *J* = 10.7, 5.3 Hz, 1H), 3.48 (dt, *J* = 11.1, 5.2 Hz, 1H), 2.68 – 2.50 (m, 2H), 1.88 (dtd, *J* = 13.7, 7.2, 6.4, 2.9 Hz, 1H), 1.78 (tdq, *J* = 11.0, 7.2, 4.5, 3.7 Hz, 1H), 1.66 – 1.50 (m, 6H), 1.38 (dd, *J* = 13.2, 6.9 Hz, 2H), 1.31 (s, 16H), 0.91 (t, *J* = 6.8 Hz, 3H). $^{13}C\{^1H\}$ NMR (100 MHz, CD_3CN) δ 81.9, 64.0, 31.6, 31.6, 31.4, 29.9, 29.9, 29.7, 29.2, 29.0, 28.9, 28.7, 28.6, 25.5, 22.4, 21.5, 13.4. HRMS (ESI-TOF) *m/z* calc[d] for $C_{17}H_{35}OS$ ($[M+H]^+$): 287.2403; found 287.2410.

1-(propylthio)isochromane (9). The reaction with substrate **8a** (102 mg, 0.620 mmol, 1 equiv.) afforded a colorless liquid (yield: 105.9 mg, 82%): IR (CH_3CN): ν_{max} (cm^{-1}) 3005, 2944, 1418, 1375, 1038, 918, 749. ^1H NMR (400 MHz, CD_3CN) δ 7.24 – 7.13 (m, 4H), 6.25 (s, 1H), 4.43 – 4.33 (m, 1H), 3.88 (ddd, *J* = 11.4, 6.4, 1.4 Hz, 1H), 3.08 – 2.96 (m, 1H), 2.81 (ddd, *J* = 13.0, 7.7, 6.6 Hz, 1H), 2.73 – 2.58 (m, 2H), 1.80 – 1.68 (m, 2H), 1.04 (t, *J* = 7.3 Hz, 3H). $^{13}C\{^1H\}$ NMR (100 MHz, CD_3CN) δ 134.9, 133.7, 128.1, 126.5, 126.4, 124.9, 82.7, 58.7, 23.0, 21.7, 13.4, 12.1. HRMS (ESI-TOF) *m/z* calc[d] for $C_{12}H_{15}OS$ ($[M-H]^-$): 207.0849; found 207.0842.

General procedure for synthesis of substrates 8b-d: DDQ (2.1 g, 9.3 mmol, 1.2 equiv.) were placed in a Schlenk flask with a stir bar and purged with N_2. The solid was then dissolved in dry CH_2Cl_2 (50 mL). The corresponding alcohol (5.0 mL) and isochroman (1.06 g, 7.91 mmol, 1.0 equiv.) was added to the flask. The reaction was stirred at room temperature in a sand bath for 24 h. The mixture was then quenched with aqueous saturated $NaHCO_3$ and filtered through celite. The aqueous layer was separated and partitioned twice with CH_2Cl_2, and the combined organic extracts were washed with aqueous saturated $NaHCO_3$ and brine. The solvent was dried over anhydrous $MgSO_4$ and removed. The products were dried *in vacuo* and purified by silica gel chromatography eluting with 0-10% EtOAc/hexane.

1-(hexyloxy)isochromane (8b). The reaction with 1-hexanol afforded a colorless oil (yield: 1.5 g, 77%): IR (CH_3CN): ν_{max} (cm^{-1}) 3164, 3005, 2944, 1442, 1375, 1038, 918, 749. ^1H NMR (400 MHz, CD_3CN) δ 7.29 – 7.25 (m, 1H), 7.24 – 7.20 (m, 2H), 7.19 – 7.15 (m, 1H), 5.54 (s, 1H), 4.08 (tdd, *J* = 11.8, 3.5, 0.6 Hz, 1H), 3.89 – 3.81 (m, 2H), 3.62 (dt, *J* = 9.6, 6.4 Hz, 1H), 2.96 (dddd, *J* = 16.6, 11.9, 6.2, 1.1 Hz, 1H), 2.65 (dddd, *J* = 16.7, 3.6, 1.7, 0.6 Hz, 1H), 1.64 (dq, *J* = 8.3, 6.6 Hz, 2H), 1.42 (dddd, *J* = 14.0, 7.3, 3.5, 1.8 Hz, 2H), 1.35 (tq, *J* = 6.7, 3.6, 2.8 Hz, 4H), 0.99 – 0.88 (m, 3H). $^{13}C\{^1H\}$ NMR (100 MHz, CD_3CN) δ 134.8, 134.3, 128.4, 127.9, 127.6, 126.0, 96.5, 67.7, 57.3, 31.5, 29.6, 27.7, 25.8, 22.5, 13.5. HRMS (ESI-TOF) *m/z* calc[d] for $C_{15}H_{21}O_2$ ($[M-H]^-$): 233.1547; found 233.1549.

1-(decyloxy)isochromane (8c). The reaction with 1-decanol afforded a colorless oil (yield: 1.8 g, 80%): IR (CH_3CN): ν_{max} (cm^{-1}) 3162, 3003, 2947, 1443, 1375, 1039, 918, 748. ^1H NMR (400 MHz, CD_3CN) δ 7.29 – 7.21 (m, 3H), 7.16 (d, *J* = 7.2 Hz, 1H), 5.54 (s, 1H), 4.17 – 4.02 (m, 1H), 3.91 – 3.77 (m, 2H), 3.62 (dt, *J* = 9.6, 6.4 Hz, 1H), 2.96 (ddd, *J* = 17.1, 11.9, 6.1 Hz, 1H), 2.71 – 2.59 (m, 1H), 1.69 – 1.60 (m, 2H), 1.37 – 1.27 (m, 12H), 0.98 – 0.89 (m, 3H). $^{13}C\{^1H\}$ NMR (100 MHz, CD_3CN) δ 134.8, 134.2, 128.4, 127.9, 127.5, 125.9, 96.5, 67.7, 57.3, 31.7, 29.6, 29.4, 29.4, 29.2, 29.1, 27.6, 26.1, 22.5, 13.5. HRMS (ESI-TOF) *m/z* calc[d] for $C_{19}H_{30}NaO_2$ ($[M+Na]^+$): 313.2143; found 313.2140.

1-(pentan-2-yloxy)isochromane (8d). The reaction with 2-pentanol afforded a colorless oil (yield: 1.4 g, 79%): IR (CH_3CN): ν_{max} (cm^{-1}) 3163, 3004, 2945, 1375, 1038, 918, 750. ^1H NMR (400 MHz, CD_3CN) δ 7.30 – 7.13 (m, 4H), 5.65 (d, *J* = 2.8 Hz, 1H), 4.12 (tt, *J* = 11.7, 3.3 Hz, 1H), 3.96 (tt, *J* = 11.3, 5.4 Hz, 1H), 3.90 – 3.82 (m, 1H), 2.95 (ddd, *J* = 17.5, 12.0, 6.1 Hz, 1H), 2.70 – 2.60 (m, 1H), 1.63 – 1.34 (m, 3H), 1.28 (dd, *J* = 6.1, 1.1 Hz, 2H), 0.94 (t, *J* = 6.7 Hz, 2H). $^{13}C\{^1H\}$ NMR (100 MHz, CD_3CN) δ 135.0, 134.4, 128.4, 127.8, 127.7, 127.5, 93.7, 71.5, 57.4, 39.4, 27.6, 21.2, 18.7, 13.3. HRMS (ESI-TOF) *m/z* calc[d] for $C_{14}H_{19}O_2$ ($[M-H]$): 219.1391; found 219.1394.

General procedure for substitution reactions. The electrophile (1 mol.-eq., 6.3 μmol, 10 μL of 0.63 M solution in CD_3CN) was placed in an NMR tube followed by 5 mol % cage 1 (0.31 μmol, 2 mg), 5 mol % CSA **2** (0.315 μmol, 10 μL of 0.0315 M solution in CD_3CN), 30 mol % control **3** (1.86 mmol, 5 μL of 0.372 M solution in CD_3CN) or 1 mol.-eq. cavity filling guest **10** (6.3 μmol, 10 μL of 0.63 M solution in CD_3CN). The nucleophile (1.25 mol.-eq., 7.9 μmol, 10 μL of 0.79 M solution in CD_3CN) was then added followed by 1,4-dioxane as the internal standard (0.5 mol.-eq., 3.2 μmol, 10 μL of 0.32 M solution in CD_3CN). A combined total volume of 400 μL of CD_3CN was added, and the tube was capped and sealed around with parafilm. The sample was quickly shaken. The reaction progress was monitored over time. An initial ^1H NMR spectrum of the reaction mixture was obtained to verify the stoichiometry of the sample. The percent conversion values were obtained via integration of the product and substrate peaks against the internal standard. Experiments were performed in triplicates.

General procedure for binding affinity calculations. A 1.5 μM solution of cage 1 was prepared in spectroscopic grade CH_3CN via dilutions from a 0.3 mM stock solution, and added to a UV-Vis cuvette. To this solution was then added 1 μL aliquots from a 4.5 mM solution of the corresponding guest molecule, equating to one molar equivalent guest to cage. These additions were continued until there was no observable change in the absorption spectrum. Binding affinities were calculated via linear regression analysis using the Nelder-Mead method from the change in absorbance at two points (300nm/330nm), the data was fit to

either a 1:1 or 1:2 binding mode.[19] See Supporting Information for titrations and fitting plots.

ASSOCIATED CONTENT

Supporting Information

NMR data of newly synthesized molecules, NMR data of catalyzed reactions and optical data, binding isotherms and curve fittings to analyze guest binding. This material is available free of charge via the Internet at http://pubs.acs.org.

AUTHOR INFORMATION

Corresponding Authors

* E-mail: richard.hooley@ucr.edu

ACKNOWLEDGMENTS

The authors would like to thank the National Science Foundation (CHE-2002619 to R.J.H. and CHE-1626673 for the purchase of Bruker NEO 600 and NEO 400 NMR spectrometers) for funding.

REFERENCES

(1) Bogie, P.M.; Miller, T.F.; Hooley, R.J. Synthesis and applications of endohedrally functionalized metal-ligand cage complexes *Isr. J. Chem.* **2019**, *59*, 130–139.

(2) Kirby, A. J. Enzyme mechanisms, models, and mimics. *Angew. Chem., Int. Ed. Engl.* **1996**, *35*, 707–724.

(3) (a) Brown, C. J.; Toste, F. D.; Bergman, R. G.; Raymond, K. N. Supramolecular catalysis in metal-ligand cluster hosts. *Chem. Rev.* **2015**, *115*, 3012–3035. (b) Dong, Z.; Luo, Q.; Liu, J. Artificial enzymes based on supramolecular scaffolds. *Chem. Soc. Rev.* **2012**, *41*, 7890–7908.

(4) (a) Rizzuto, F. J.; von Krbek, L. K. S.; Nitschke, J. R. Strategies for binding multiple guests in metal-organic cages. *Nat. Rev. Chem.* **2019**, *3*, 204–222. (b) a) Rizzuto, F. J.; Carpenter, J. P.; Nitschke, J. R. Multisite binding of drugs and natural products in an entropically favorable, heteroleptic receptor. *J. Am. Chem. Soc.* **2019**, *141*, 9087–9095.

(5) Hof, F.; Craig, S. L.; Nuckolls, C.; Rebek, J., Jr. Molecular encapsulation. *Angew. Chem., Int. Ed.* **2002**, *41*, 1488–1508.

(6) (a) Cram, D. J. Nobel prize lecture: the design of molecular host, guests, and their complexes *Angew. Chem., Int. Ed. Engl.* 1988, *27*, 1009–1020. (b) Kang, J. M.; Rebek, J., Jr. Acceleration of a Diels-Alder reaction by a self-assembled molecular capsule. *Nature* **1997**, *385*, 50–52. (c) Chen, J.; Rebek, J., Jr. Selectivity in an encapsulated cycloaddition reaction. *Org. Lett.* **2002**, *4*, 327–329.

(7) (a) Fiedler, D.; Bergman, R. G.; Raymond, K. N. Supramolecular catalysis of a unimolecular transformation: Aza-cope rearrangement within a self-assembled host. *Angew. Chem., Int. Ed.* **2004**, *43*, 6748–6755. (b) Yoshizawa, M.; Tamura, M.; Fujita, M. Diels-Alder in aqueous molecular hosts: Unusual regioselectivity and efficient catalysis. *Science* **2006**, *312*, 251–254. (c) Nishioka, Y.; Yamaguchi, T.; Yoshizawa, M.; Fujita, M. Unusual [2+4] and [2+2] cycloadditions of arenes in the confined cavity of self-assembled cages. *J. Am. Chem. Soc.* **2007**, *129*, 7000–7001. (d) Martí-Centelles, V.; Lawrence, A. L.; Lusby, P. J. High activity and efficient turnover by a simple, self-assembled artificial Diels-Alderase. *J. Am. Chem. Soc.* **2018**, *140*, 2862–2868.

(8) Pluth, M. D.; Bergman, R. G.; Raymond, K. N. Acid catalysis in basic solution: A supramolecular host promotes orthoformate hydrolysis. *Science.* **2007**, *316*, 85–88.

(9) Cullen, W.; Metherell, A. J.; Wragg, A. B.; Taylor, C. G. P.; Williams, N. H.; Ward, M. D. Catalysis in a cationic coordination cage using a cavity-bound guest and surface-bound anions: inhibition, activation, and autocatalysis. *J. Am. Chem. Soc.* **2018**, *140*, 2821–2828.

(10) (a) Wang, J. Z.; Brown, C. J.; Bergman, R. G.; Raymond, K. N; Toste, F. D. Hydroalkoxylation catalyzed by a gold(I) complex encapsulated in a supramolecular host. *J. Am. Chem. Soc.* **2011**, *133*, 7358–7360. (b) Levin, M. D.; Kaphan, D. M.; Hong, C. M.; Bergman, R. G.; Raymond, K. N.; Toste, F. D. Scope and mechanism of cooperativity at the intersection of organometallic and supramolecular catalysis. *J. Am. Chem. Soc.* **2016**, *138*, 9682–9693.

(11) (a) Bolliger, J. L.; Belenguer, A. M.; Nitschke, J. R. Enantiopure water-soluble $[Fe_4L_6]$ cages: host–guest chemistry and catalytic activity. *Angew. Chem. Int. Ed.* **2013**, *52*, 7958–7962. (b) Roy, B.; Devaraj, A.; Saha, R.; Jharimune, S.; Chi, K.-W.; Mukherjee, P. S. Catalytic intramolecular cycloaddition reactions by using a discrete molecular architecture. *Chem. – Eur. J.* **2017**, *23*, 15704–15712. c) Dai, F.-R.; Zhang, L.; Li, J.; Lin, W.; Wang, Z. Switching on supramolecular catalysis via cavity mediation and electrostatic regulation. *Angew. Chem. Int. Ed.* **2016**, *55*, 12778–12782. (d) Bender, T.A.; Bergman, R. G.; Raymond, K. N.; Toste, F. D. A supramolecular strategy for selective catalytic hydrogenation independent of remote chain length. *J. Am. Chem. Soc.* **2019**, *141*, 11806–11810. (e) Hong, T.; Zhang, Z.; Sun, Y.; Tao, J.-J.; Tang, J.-D.; Xie, C.; Wang, M.; Chen, F.; Xie, S.-S.; Li, S.; Stang, P.J. Chiral metallacycles as catalysts for asymmetric conjugate addition of styrylboronic acids to α,β-enones. *J. Am. Chem. Soc.* **2020**, *142*, 10244–10249.

(12) (a) Kaphan, D. M.; Levin, M. D.; Bergman, R. G.; Raymond, K. N.; Toste, F. D. A supramolecular microenvironment strategy for transition metal catalysis. *Science* **2015**, *350*, 1235–1238. (b) Cullen, W.; Misuraca, M. C.; Hunter, C. A.; Williams, N. H.; Ward, M. D. Highly efficient catalysis of the Kemp elimination in the cavity of a cubic coordination cage. *Nat. Chem.* **2016**, *8*, 231–236.

(13) Hooley, R. J.; Biros, S. M.; Rebek, J., Jr. A deep, water-soluble cavitand acts as a phase-transfer catalyst for hydrophobic species. *Angew. Chem., Int. Ed.* **2006**, *45*, 3517–3519.

(14) (a) Harris, K.; Fujita, D.; Fujita, M. Giant hollow M_nL_{2n} spherical complexes: structure, functionalisation and applications. *Chem. Commun.* **2013**, *49*, 6703–6712. (b) Zhang, Q.; Catti, L.; Tiefenbacher, K. Catalysis inside the hexameric resorcinarene capsule. *Acc. Chem. Res.* **2018**, *51*, 2107–2114.

(15) (a) Gramage-Doria, R.; Hessels, J.; Leenders, S. H. A. M.; Tröppner, O.; Dürr, M.; Ivanović-Burmazović, I.; Reek, J. N. H. Gold(I) catalysis at extreme concentrations inside self-assembled nanospheres *Angew. Chem., Int. Ed.* **2014**, *53*, 13380–13384. (b) Wang, Q.-Q.; Gonell, S.; Leenders, S. H. A. M.; Dürr, M.; Ivanović-Burmazović, I.; Reek, J. N. H. Self-assembled nanospheres with multiple endohedral binding sites pre-organize catalysts and substrates for highly efficient reactions. *Nat. Chem.* **2016**, *8*, 225–230. (c) Braüer, T. M.; Zhang, Q.; Tiefenbacher, K. Iminium catalysis inside a self-assembled supramolecular capsule: Modulation of enantiomeric ex-

cess. *Angew. Chem., Int. Ed.* **2016**, 55, 7698–7701. (d) Catti, L.; Tiefenbacher, K. Brønsted acid-catalyzed carbonyl-olefin metathesis inside a self-assembled supramolecular host. *Angew. Chem., Int. Ed.* **2018**, *57*, 14589–14592. (e) Zhang, Q.; Tiefenbacher, K. Terpene cyclization catalyzed inside a self-assembled cavity. *Nat. Chem.* **2015**, *7*, 197–202. (f) Zhang, Q.; Catti, L.; Pleiss, J.; Tiefenbacher, K. Terpene cyclizations inside a supramolecular catalyst: Leaving-group-controlled product selectivity and mechanistic studies. *J. Am. Chem. Soc.* **2017**, *139*, 11482–11492.

(16) (a) Holloway, L. R.; Bogie, P. M.; Lyon, Y.; Ngai, C.; Miller, T. F.; Julian, R.R.; Hooley, R.J. Tandem reactivity of a self-assembled cage catalyst with endohedral acid groups. *J. Am. Chem. Soc.* **2018**, *140*, 8078–8081. (b) Bogie, P. M.; Holloway, L. R.; Ngai, C.; Miller, T. F.; Grewal, D. K.; Hooley, R. J. A self-assembled cage with endohedral acid groups both catalyzes substitution reactions and controls their molecularity. *Chem. Eur. J.* **2019**, *25*, 10232–10238. (c) Ngai, C.; Sanchez-Marsetti, C. M.; Harman, W.H.; Hooley, R.J. Supramolecular Catalysis of the oxa-Pictet-Spengler Reaction with an Endohedrally Functionalized Self-Assembled Cage Complex. *Angew. Chem. Int. Ed.* **2020**, *59*, 23505–23509. (d) Ngai, C.; Bogie, P.M.; Holloway, L.R.; Dietz, P.C.; Mueller, L.J.; Hooley, R.J. Cofactor-mediated nucleophilic substitution catalyzed by a self-assembled holoenzyme mimic. *J. Org. Chem.* **2019**, *84*, 12000–12008.

(17) (a) Brown, H.C. et al., in Braude, E.A. and F.C. Nachod *Determination of Organic Structures by Physical Methods*, Academic Press, New York, 1955; (b) Dippy, J. F. J.; Hughes, S. R. C.; Rozanski, A. The dissociation constants of some symmetrically disubstituted succinic acids. *J. Chem. Soc.* **1959**, 2492–2498.

(18) Deno, N.C.; Turner, J.O. The basicity of alcohols and ethers. *J. Org. Chem.* **1966**, *31* 1969–1970.

(19) Association constants calculated using BindFit software found at http://supramolecular.org. (a) Hibbert, D. B.; Thordarson, P. The death of the Job plot, transparency, open science and online tools, uncertainty estimation methods and other developments in supramolecular chemistry data analysis. *Chem. Commun.* **2016**, *52*, 12792–12805. (b) Thordarson, P. Determining association constants from titration experiments in supramolecular chemistry. *Chem. Soc. Rev.* **2011**, *40*, 1305–1323.

(20) Tiedemann, B. E. F.; Raymond, K. N. Dangling arms: a tetrahedral supramolecular host with partially encapsulated guests. *Angew. Chem. Int. Ed.* **2006**, *45*, 83–86.

(21) Zhang, J. J.; Yan, C.S.; Peng, Y.; Luo, Z.B.; Xu, X.B.; Wang Y. W. Total synthesis of (±)-sacidumlignans D and A through Ueno–Stork radical cyclization reaction. *Org. Biomol. Chem.* **2013**, *11*, 2498–2513.

(22) Banda, F. M.; Brettle, R. Anodic oxidation. Part 16. A comparison of chemical and electrochemical routes to alkyl diphenylallyl ethers. *J. Chem. Soc. Perkin Trans.* **1977**, *15*, 1773–1776.

(23) Reisman, S. E.; Doyle, A. G.; Jacobsen, E. N. Enantioselective thiourea-catalyzed additions to oxocarbenium ions. *J. Am. Chem. Soc.* **2008**. *130*, 7198–7199.

(24) Miller, E. M.; Walczak, M. A. Copper-catalyzed oxidative acetalization of boronic esters: an umpolung strategy for cyclic acetal synthesis. *J. Org. Chem.* **2020**, *85*, 8230–8239.

(25) Kang, S. K.; Jung, K. Y.; Park, C. H.; Jang, S. B. Palladium-catalyzed coupling of allylic cyclic carbonates with iodobenzene and hypervalent iodonium salts. *Tetrahedron Lett.* **1995**, *36*, 8047–8050.

(26) (a) Silveira, C. C.; Mendes, S. R.; Líbero, F. M. Solvent-free anti-Markovnikov addition of thiols to alkenes using anhydrous cerium (III) chloride as catalyst. *Synlett*. **2010**, *5*, 790–792. (b) Kipnis, F.; Ornfelt, J. 2-Substituted tetrahydropyranyl sulfides. *J. Am. Chem. Soc.* **1951**, *73*, 822–822.

(27) Block, E.; Aslam, M. [[(2-Tetrahydrofuranyl)-and (2-tetrahydropyranyl) thio] methyl] lithium: methanethiol carbanion equivalents. *J. Am. Chem. Soc.* **1985**, *107*, 6729–6731.

(28) Kimura, M.; Shimizu, M.; Tanaka, S.; Tamaru, Y. Pd-catalyzed nucleophilic allylic alkylation of aliphatic aldehydes by the use of allyl alcohols. *Tetrahedron*. **2005**, *61*, 3709–3718.